On the spectrum of fluctuations of a liquid surface: From the molecular scale to the macroscopic scale

Edgar M. Blokhuis

On the spectrum of fluctuations of a liquid surface: From the molecular scale to the macroscopic scale

Edgar M. Blokhuis[a)]

Colloid and Interface Science, Leiden Institute of Chemistry, Gorlaeus Laboratories, P.O. Box 9502, 2300 RA Leiden, The Netherlands

We show that to account for the full spectrum of surface fluctuations from low scattering vector $qd \ll 1$ (classical capillary wave theory) to high $qd \gtrsim 1$ (bulklike fluctuations), one must take account of the interface's bending rigidity at intermediate scattering vector $qd \lesssim 1$, where d is the molecular diameter. A molecular model is presented to describe the bending correction to the capillary wave model for short-ranged and long-ranged interactions between molecules. We find that the bending rigidity is negative when the Gibbs equimolar surface is used to define the location of the fluctuating interface and that on approach to the critical point it vanishes proportionally to the interfacial tension. Both features are in agreement with Monte Carlo simulations of a phase-separated colloid-polymer system. © *2009 American Institute of Physics.* [DOI: 10.1063/1.3054346]

I. INTRODUCTION

The description of the spectrum of surface fluctuations of a liquid from the macroscopic scale down to the molecular scale remains a challenging experimental and theoretical problem. Using grazing incidence light scattering experiments, Daillant and co-workers[1] were able, for the first time, to determine the full spectrum of surface fluctuations, where in previous experiments (ellipsometry and reflectivity) only certain aspects of the spectrum could be determined. At the same time, the spectrum can now be analyzed in computer simulations with ever increasing accuracy.[2–4]

Theoretical insight into the structure of a simple liquid surface is provided by density functional theories (DFTs) on the one hand[5–7] and the capillary wave (CW) model on the other hand.[8–10] DFTs provide a description of the interface on a microscopic level. The prototype of such theories, the van der Waals squared-gradient model, was very successful in describing, for the first term, the density profile and surface tension in terms of molecular parameters.[7] It, however, fails to capture the subtle role of long wavelength interfacial fluctuations described by the CW model.[8–10]

The CW model introduced in 1965 (Ref. 8) describes the spectrum of fluctuations in terms of a height function $h(\vec{r}_{\parallel})$ with the surface tension σ and gravity g acting as the dominant restoring forces. The length scale involved in describing CWs is the capillary length, $L_c \equiv \sqrt{\sigma/(m\Delta\rho g)}$, which may be as large as a tenth of a millimeter. The theoretical challenge is to incorporate both theories and to describe the spectrum of fluctuations of a liquid surface, as determined from light scattering experiments and computer simulations, from the molecular scale to the scale of CWs.

An important ingredient in "bridging the gap" between CWs and the molecular scale is an extension of the CW model that incorporates the energy associated with *bending* the interface.[11–13] Bending is important when the wavelength

of the height fluctuations is approximately $\sqrt{k_{\mathrm{B}}T/\sigma}$, which is typically of the order of a few times the molecular diameter, i.e., close to the scale where the molecular structure becomes important and the density fluctuations are more bulklike. The natural question that arises is whether it is possible to describe the full spectrum of surface fluctuations by the CW model at long wavelengths and bulklike fluctuations at the molecular scale. Is it then necessary to include the leading order correction to the CW model from bending or are even higher order terms, relevant at even smaller length scales, required?

This article addresses these questions in two parts (a condensed version has appeared in Ref. 14). In the first part, we analyze the spectrum of fluctuations recently obtained by Vink *et al.*[3] in computer simulations of a phase-separated polymer-colloid system[15–18] in which the interactions are strictly short ranged (SR). It is shown that the simulation data are very accurately described by the combination of the CW model extended to include a bending correction, with the bending rigidity as an adjustable parameter, and bulklike fluctuations.

In the second part, a molecular basis for the bending correction to the CW model is offered and the results are compared with the simulations. The theoretical framework used for the comparison is mean-field DFT in which the interactions are described by a nonlocal integral term.[5–7,19] The advantage of this approach is that it features the full shape of the interaction potential enabling the analysis of different forms and ranges of the interaction potential. We consider both SR interactions and long-ranged (LR) interactions, which fall of as $U(r) \propto 1/r^6$ at large intermolecular separations.

An important ingredient in our theoretical analysis is the modification of the density profile, described by $\rho_1(z)$, due to the local bending of the interface.[20] The determination of $\rho_1(z)$ requires one to formulate precisely the thermodynamic conditions used to vary the interfacial curvature. Several ap-

---

a)Electronic mail: e.blokhuis@chem.leidenuniv.nl.

proaches for the determination of $\rho_1(z)$ have appeared in literature.[19–22] They differ in the form of the external field used to set the curvature to a specific value; in the equilibrium approach[20] the external field is uniform throughout the system, whereas in the approach by Parry and Boulter[21] and Blokhuis et al.[22] it is infinitely sharp-peaked ($V_{ext} \propto \delta(z)$) at the interface. In this article we suggest to add an external field acting in the interfacial region only with a peak width of the order of the thickness of the interfacial region. The advantage of this approach is that the bulk regions are unaffected by the addition of the external field and the resulting $\rho_1(z)$ is a continuous function.

Our paper is organized as follows: In Sec. II, the general form of the surface structure factor to describe the spectrum of interfacial fluctuations is derived as the combination of the CW model extended to include a bending correction and bulklike fluctuations. This form is then compared in Sec. III to the Monte Carlo (MC) simulation results by Vink et al.[3] for the phase-separated polymer-colloid system. In Sec. IV, the mean-field DFT used to provide a molecular basis for the bending extension to the CW model is presented. Explicit results are obtained for SR interactions (Sec. V) and LR interactions (Sec. VI). We end with a discussion of results.

II. THE FLUCTUATING LIQUID SURFACE

In the classical CW model, the fluctuating interface is described by a two-dimensional surface height function $h(\vec{r}_\parallel)$, where $\vec{r}_\parallel = (x, y)$ is the direction parallel to the surface.[8–10] The fluctuating density profile can then be written in terms of an "intrinsic density profile" shifted over a distance $h(\vec{r}_\parallel)$ as follows:

$$\rho(\vec{r}) = \rho_0(z - h(\vec{r}_\parallel)), \tag{1}$$

where $\rho_0(z)$ is the intrinsic density profile. Often, fluctuations are assumed to be small so that an expansion in h can be made, neglecting terms of $\mathcal{O}(h^2)$,

$$\rho(\vec{r}) = \rho_0(z) - \rho_0'(z) h(\vec{r}_\parallel) + \cdots. \tag{2}$$

An important consequence of the above linearization is that one may now identify the intrinsic density profile as the *average* density profile, $\rho_0(z) = \langle \rho(\vec{r}) \rangle$, in view of the fact that $\langle h(\vec{r}_\parallel) \rangle = 0$. It is convenient to locate the $z = 0$ plane such that it coincides with the Gibbs equimolar surface,[7,23] i.e.,

$$\int_{-\infty}^{\infty} dz [\langle \rho(\vec{r}) \rangle - \rho_{step}(z)] = \int_{-\infty}^{\infty} dz [\rho_0(z) - \rho_{step}(z)] = 0, \tag{3}$$

where $\rho_{step}(z) = \rho_\ell \Theta(-z) + \rho_v \Theta(z)$ with $\Theta(z)$ the Heaviside function and $\rho_{\ell,v}$ the bulk density in the liquid and vapor regions, respectively.

In the above model for $\rho(\vec{r})$, the density correlations are essentially given by the correlations of $h(\vec{r}_\parallel)$, which are described by the height-height correlation function

$$S_{hh}(r_\parallel) \equiv \langle h(\vec{r}_{1,\parallel}) h(\vec{r}_{2,\parallel}) \rangle, \tag{4}$$

where $\vec{r}_\parallel \equiv \vec{r}_{2,\parallel} - \vec{r}_{1,\parallel}$ and $r_\parallel \equiv |\vec{r}_\parallel|$.

To determine the height-height correlation function, one should examine the change in free energy, $\Delta\Omega$, associated with a fluctuation of the interface. In the CW model it is described by considering the change in free energy associated with a distortion of the surface against gravity and surface area extension,[8]

$$\Delta\Omega = \frac{1}{2} \int d\vec{r}_\parallel [m\Delta\rho g h(\vec{r}_\parallel)^2 + \sigma |\vec{\nabla} h(\vec{r}_\parallel)|^2]. \tag{5}$$

It is convenient to express $\Delta\Omega$ in terms of the Fourier Transform of $h(\vec{r}_\parallel)$, $h(\vec{q}) = \int d\vec{r}_\parallel e^{-i\vec{q}\cdot\vec{r}_\parallel} h(\vec{r}_\parallel)$,

$$\Delta\Omega = \frac{1}{2} \int \frac{d\vec{q}}{(2\pi)^2} [m\Delta\rho g + \sigma q^2] h(\vec{q}) h(-\vec{q}). \tag{6}$$

In the CW model the height-height correlation function is determined by a full statistical mechanical analysis[9,10] in which the above expression for the change in free energy is interpreted as the so-called CW Hamiltonian, $\Delta\Omega = \mathcal{H}_{CW}[h(\vec{r}_\parallel)]$. In general, one has

$$S_{hh}(r_\parallel) = \frac{1}{Z} \int \mathcal{D}h \, h(\vec{r}_{1,\parallel}) h(\vec{r}_{2,\parallel}) e^{-\mathcal{H}_{CW}[h]/k_B T}, \tag{7}$$

where Z is the partition function associated with $\mathcal{H}_{CW}[h]$, k_B is Boltzmann's constant, and T is the temperature. It can be shown that[9,10]

$$S_{hh}(q) = \int d\vec{r}_\parallel e^{-i\vec{q}\cdot\vec{r}_\parallel} S_{hh}(r_\parallel) = \frac{k_B T}{m\Delta\rho g + \sigma q^2} = \frac{k_B T}{\sigma(L_c^{-2} + q^2)}. \tag{8}$$

For simplicity, we ignore gravity effects in the following and set $L_c = \infty$ ($g = 0$).

A. Extended capillary wave model

In the derivation of the classical CW model, one assumes an expansion in gradients of $h(\vec{r}_\parallel)$, $|\vec{\nabla} h| \ll 1$. In the *extended* capillary wave (ECW) model, one wishes to extend the expansion by including higher derivatives of $h(\vec{r}_\parallel)$. To leading order one may then write the fluctuating density as[19,22]

$$\rho(\vec{r}) = \rho_0(z) - \rho_0'(z) h(\vec{r}_\parallel) - \frac{\rho_1(z)}{2} \Delta h(\vec{r}_\parallel) + \cdots. \tag{9}$$

The function $\rho_1(z)$ is identified as the correction to the density profile due to the *curvature* of the interface, $\Delta h(\vec{r}_\parallel) \approx -1/R_1 - 1/R_2$, with R_1 and R_2 the (principal) radii of curvature. The prefactor of $-1/2$ is chosen such that the notation is consistent with an analysis in which the curvature does not result from a fluctuation of the planar interface, but is due to the fact that one considers a spherical liquid droplet ($R_1 = R_2 = R$) in (metastable) equilibrium with a bulk vapor phase.[20,24,25] An expansion in the curvature of the density profile $\rho_s(r)$ then gives

$$\rho_s(r) = \rho_0(r) + \frac{\rho_1(r)}{R} + \cdots, \tag{10}$$

which parallels the expansion in Eq. (9).

The inclusion of curvature corrections in the ECW model leads to higher order terms in an expansion in q^2, terms beyond σq^2, in the expression for $\Delta\Omega$ in Eq. (6). It is customary to capture these higher order terms by introducing a wave vector dependent surface tension $\sigma(q)$ as follows:[12]

$$\Delta\Omega = \frac{1}{2}\int \frac{d\vec{q}}{(2\pi)^2}\sigma(q)q^2 h(\vec{q})h(-\vec{q}), \tag{11}$$

which gives for the height-height correlation function

$$S_{hh}(q) = \frac{k_B T}{\sigma(q)q^2}. \tag{12}$$

The precise form of $\sigma(q)$ depends sensitively on the behavior of the interaction potential at large distances.[19] When the interaction potential is sufficiently SR, the expansion of $\sigma(q)$ in q^2 is regular and the leading correction is of the form

$$\sigma(q) = \sigma + kq^2 + \mathcal{O}(q^4) \quad \text{(SR)}. \tag{13}$$

The coefficient k is identified as the *bending rigidity*.[11–13] This is because the form for $\Delta\Omega$ in Eq. (11), with $\sigma(q)$ given by Eq. (13), can also be derived from the Helfrich free energy expression,[11] which reads for a fluctuating interface

$$\Delta\Omega = \frac{1}{2}\int d\vec{r}_\parallel[\sigma|\vec{\nabla}h(\vec{r}_\parallel)|^2 + k(\Delta h(\vec{r}_\parallel))^2]. \tag{14}$$

When the interaction potential is LR, specifically when it falls of as $U(r) \propto 1/r^6$ at large intermolecular distances, which is the case for regular fluids due to London-dispersion forces, one finds that the leading correction to $\sigma(q)$ picks up a logarithmic contribution[19]

$$\sigma(q) = \sigma + k_s q^2 \ln(q\ell_k) + \mathcal{O}(q^4) \quad \text{(LR)}, \tag{15}$$

with k_s and ℓ_k parameters independent of q. The coefficient k_s depends on the asymptotic behavior of $U(r)$ but is otherwise a *universal* constant.[19] The bending length ℓ_k depends, like the bending rigidity k, on the microscopic parameters of the model. In principal, all the parameters σ, k, k_s, and ℓ_k can be expressed in terms of the density profiles $\rho_0(z)$ and $\rho_1(z)$ by inserting the fluctuating density as given in Eq. (9) into a microscopic model for the free energy and comparing the result with Eq. (11).

It is important to realize that the ECW model assumes a curvature expansion in Eq. (9), which translates into an expansion in q^2 in Eq. (11) that is valid only up to $\mathcal{O}(q^4)$. Higher order terms are not systematically included. The result is that one should limit the expansion of $\sigma(q)$ in Eq. (13) or Eq. (15) to the order in q indicated.

B. Definition of the height profile

An important subtlety in the preceding analysis is the fact that the location of the interface, i.e., the value of the height function $h(\vec{r}_\parallel)$, cannot be defined *unambiguously*.[23] A certain procedure must always be formulated to determine $h(\vec{r}_\parallel)$. It turns out that the choice for $h(\vec{r}_\parallel)$ influences the density profile $\rho_1(z)$, which, in turn, determines the value of the bending parameters k and ℓ_k.

We explicitly consider two canonical choices for the determination of $h(\vec{r}_\parallel)$; the *crossing* constraint (cc) and the *in-tegral* constraint (ic).[21,22] Other choices are certainly possible and equally legitimate as long as they lead to a location of the dividing surface that is "sensibly coincident" with the interfacial region.[23] In this context we like to mention the work by Tarazona *et al.*,[4] who define the location of the interface based on the distribution of molecules rather than the molecular density alone.

In the cc, $h(\vec{r}_\parallel)$ is defined as the height where the fluctuating density equals some fixed value of the density that lies in between the limiting bulk densities, say, $\rho(\vec{r}) = \rho_0(z=0)$,

$$\rho(\vec{r}_\parallel, z = h(\vec{r}_\parallel)) = \rho_0(0) \quad \text{(cc)}. \tag{16}$$

Using this condition in Eq. (9), one finds the following constraint for $\rho_1(z) = \rho_1^{cc}(z)$:

$$\rho_1^{cc}(0) = 0. \tag{17}$$

In the ic, $h(\vec{r}_\parallel)$ is defined by the integral over the fluctuating density[23]

$$h(\vec{r}_\parallel) = \frac{1}{\Delta\rho}\int_{-\infty}^{\infty} dz[\rho(\vec{r}) - \rho_{step}(z)] \quad \text{(ic)}. \tag{18}$$

With this condition inserted into Eq. (9), one now finds that $\rho_1(z) = \rho_1^{ic}(z)$ is subject to the following constraint:

$$\int_{-\infty}^{\infty} dz\rho_1^{ic}(z) = 0. \tag{19}$$

We show in Sec. IV that the ambiguity in locating the dividing surface translates into the density profile $\rho_1(z)$ being determined up to an additive factor proportional to $\rho_0'(z)$.[22] In particular, $\rho_1^{ic}(z)$ and $\rho_1^{cc}(z)$ are related to

$$\rho_1^{ic}(z) = \rho_1^{cc}(z) + \alpha\rho_0'(z). \tag{20}$$

The value of the constant α can be determined by integrating both sides of the above equation over z,

$$\alpha = \frac{1}{\Delta\rho}\int_{-\infty}^{\infty} dz\rho_1^{cc}(z). \tag{21}$$

One may further show that the ambiguity in the determination of $\rho_1(z)$ is of influence to the value of the bending parameters k and ℓ_k. In Sec. IV we show that because $\rho_1^{ic}(z)$ and $\rho_1^{cc}(z)$ are related to Eq. (20), we have for the bending parameters[22]

$$k^{ic} = k^{cc} - \alpha\sigma,$$

$$k_s \ln(\ell_k^{ic}) = k_s \ln(\ell_k^{cc}) - \alpha\sigma. \tag{22}$$

Naturally, all experimentally measurable quantities *cannot* depend on the choice made for the location of the height function $h(\vec{r}_\parallel)$. The implication is that it is necessary to formulate precisely the quantity that is determined experimentally and verify that its value is independent of the choice for $h(\vec{r}_\parallel)$. This is explicitly shown next.

The quantity studied in experiments and simulations is the (surface) density-density correlation function. It is an integral into the bulk region to a certain depth L of the density-density correlation function

$$S(r_\parallel) \equiv \frac{1}{(\Delta\rho)^2} \int_{-L}^{L} dz_1 \int_{-L}^{L} dz_2 \langle [\rho(\vec{r}_1) - \rho_{\text{step}}(z_1)]$$
$$\times [\rho(\vec{r}_2) - \rho_{\text{step}}(z_2)] \rangle. \tag{23}$$

When we insert the general expression for $\rho(\vec{r})$ as given by Eq. (9) into Eq. (23), one finds that

$$S(r_\parallel) = \langle h(\vec{r}_{1,\parallel}) h(\vec{r}_{2,\parallel}) \rangle - \frac{1}{\Delta\rho} \int_{-\infty}^{\infty} dz \rho_1(z) \langle h(\vec{r}_{1,\parallel}) \Delta h(\vec{r}_{2,\parallel}) \rangle, \tag{24}$$

where we can neglect a term $\langle \Delta h \Delta h \rangle$ to the order in the curvature expansion considered. Furthermore, we have assumed that L is sufficiently large so that we can approximate

$$\int_{-L}^{L} dz \rho_0'(z) \approx -\Delta\rho,$$
$$\int_{-L}^{L} dz \rho_1(z) \approx \int_{-\infty}^{\infty} dz \rho_1(z). \tag{25}$$

Rather than $S(r_\parallel)$, we consider its Fourier transform, $S(q)$, which we shall term the *surface structure factor*,

$$S(q) = \int d\vec{r}_\parallel e^{-i\vec{q}\cdot\vec{r}_\parallel} S(r_\parallel)$$
$$= S_{hh}(q) + \frac{1}{\Delta\rho} \int_{-\infty}^{\infty} dz \rho_1(z) q^2 S_{hh}(q). \tag{26}$$

We now verify that $S(q)$ is *independent* of the choice for $h(\vec{r}_\parallel)$ by determining $S(q)$ using both the ic and cc. For simplicity, we consider the case of SR forces only (the verification for the case of LR forces follows analogously). The surface structure factor using both constraints is given by

$$S^{cc}(q) = \frac{k_B T}{\sigma q^2 + k^{cc} q^4 + \cdots} + \frac{\alpha k_B T q^2}{\sigma q^2 + k^{cc} q^4 + \cdots}$$
$$= \frac{k_B T}{\sigma q^2} - \frac{k_B T k^{cc}}{\sigma^2} + \frac{\alpha k_B T}{\sigma} + \mathcal{O}(q^2),$$
$$S^{ic}(q) = \frac{k_B T}{\sigma q^2 + k^{ic} q^4 + \cdots} = \frac{k_B T}{\sigma q^2} - \frac{k_B T k^{ic}}{\sigma^2} + \mathcal{O}(q^2), \tag{27}$$

where we have used the explicit expression for $S_{hh}(q)$ in Eq. (12) together with Eq. (13). On account of the fact that $k^{ic} = k^{cc} - \alpha\sigma$, one finds that $S^{cc}(q) = S^{ic}(q) \equiv S(q)$ as required.

This analysis shows that $S(q)$ equals the height-height correlation function when the *integral constraint* is used to define the location of the height profile, i.e.,

$$S(q) = S_{hh}^{ic}(q). \tag{28}$$

It is therefore convenient, but by no means necessary, to use the ic to define the location of the dividing surface.

Finally, we consider the contribution of "bulklike" fluctuations to the fluctuating density profile, which are predominantly present at short wavelengths, $qd \gtrsim 1$.
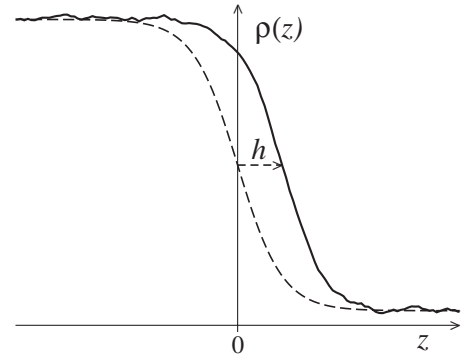

FIG. 1. Sketch of the fluctuating density profile as a function of z; the height $h = h(\vec{r}_\parallel)$ is the distance over which the intrinsic density profile $\rho_0(z)$ (dashed line) is shifted.

C. Bulklike fluctuations

Adding short wavelength, bulklike fluctuations to the fluctuating density, the full picture that emerges for $\rho(\vec{r})$ is that schematically depicted in Fig. 1. It can be described as

$$\rho(\vec{r}) = \rho_0(z) - \rho_0'(z) h(\vec{r}_\parallel) - \frac{\rho_1(z)}{2} \Delta h(\vec{r}_\parallel) + \delta\rho_b(\vec{r}), \tag{29}$$

where $\delta\rho_b(\vec{r})$ represents the bulklike fluctuations. We shall consider only small fluctuations so that $\langle \delta\rho_b \rangle = 0$ and assume that there are no correlations between height fluctuations and bulklike fluctuations, $\langle h \delta\rho_b \rangle = 0$. When we insert the expression for $\rho(\vec{r})$ as given by Eq. (29) into the expression for $S(r_\parallel)$ in Eq. (23), one finds that

$$S(r_\parallel) = S_{hh}^{ic}(r_\parallel) + \frac{1}{(\Delta\rho)^2} \int_{-L}^{L} dz_1 \int_{-\infty}^{\infty} dz_{12} \langle \delta\rho_b(\vec{r}_1) \delta\rho_b(\vec{r}_2) \rangle. \tag{30}$$

Here we have made a further approximation by replacing the integration over z_2 from $-L$ to L with an integral over z_{12} from $-\infty$ to ∞. The integral over z_1 that is left gives rise to a term that increases linearly with L. That means that the bulklike contributions to $S(r_\parallel)$ eventually dominate the height fluctuations when L becomes larger. To study surface fluctuations via $S(r_\parallel)$ it is therefore important that on the one hand L is sufficiently large in order to make the approximations in, e.g., Eq. (25) but on the other hand not so large as to completely dominate the contribution from surface height fluctuations. In Sec. III we show how these two conditions pan out for the circumstances under which the simulation results are obtained.

A further issue is that the bulk density correlation function $\langle \delta\rho_b \delta\rho_b \rangle$ differs in either phase (liquid or vapor). When one then considers the integral over z_1, it seems appropriate to approximate $\langle \delta\rho_b \delta\rho_b \rangle$ by the density correlation function in the *bulk liquid* region

$$\langle \delta\rho_b(\vec{r}_1) \delta\rho_b(\vec{r}_2) \rangle = \rho_\ell^2 [g_\ell(r) - 1] + \rho_\ell \delta(\vec{r}_{12}), \tag{31}$$

and introduce an L-dependent prefactor $\mathcal{N}_L$ to account for the integral over z_1. The surface structure factor thus becomes

$$S(q) = S_{hh}^{ic}(q) + \mathcal{N}_L S_b(q), \tag{32}$$

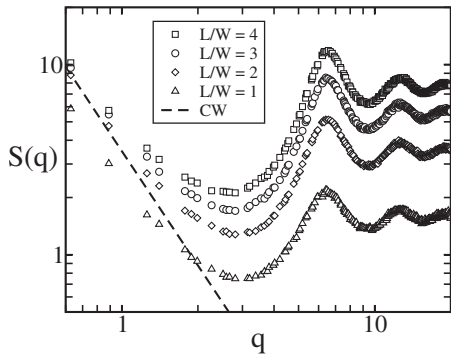with the bulk structure factor $S_b(q)$ defined as

FIG. 2. MC results by Vink *et al.* (Ref. [3]) for the surface structure factor (in units of d^4) vs q (in units of $1/d$) for various values of the integration limit $L/W = 1, 2, 3, 4$. The dashed line is the CW model. In this example, $\varepsilon = 1.8$, $\eta_p = 1.0$, and the colloidal particles are used to define z_G.
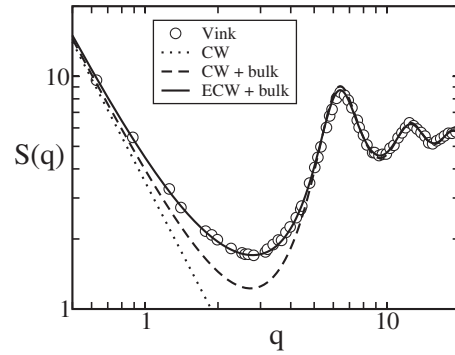

FIG. 3. MC results by Vink *et al.* (Ref. [3]) for the surface structure factor (in units of d^4) vs q (in units of $1/d$). The dotted line is the CW model, the dashed line is the combination of the CW model and the bulk correlation function, and the drawn line is the combination of the ECW model and the bulk correlation function. In this example, $\varepsilon = 1.8$, $\eta_p = 1.0$, $L/W = 3$, and the colloidal particles are used to define z_G.

$$S_b(q) = 1 + \rho_\ell \int d\vec{r}_{12} e^{-i\vec{q}\cdot\vec{r}_{12}}[g_\ell(r) - 1]. \tag{33}$$

This approximation may be justified by arguing that close to the critical point there is no distinction between the two bulk correlation functions, whereas far from the critical point the contribution from the bulk vapor can be neglected since $\rho_v \approx 0$.

The value for the L-dependent prefactor $\mathcal{N}_L$ may be determined from a fit to the limiting behavior of $S(q)$ at $q \to \infty$. For an explicit evaluation of $S_b(q)$, we have taken for $g_\ell(r)$ the Percus–Yevick (PY) solution[26] for the hard-sphere correlation function, $g_\ell(r) = g_{hs}^{PY}(r; \rho_\ell)$.

III. COMPARISON WITH MONTE CARLO SIMULATIONS

In this section, the surface structure factor in Eq. (32) is compared to the results from MC simulations by Vink *et al.*[3] The system considered consists of a mixture of colloidal particles with diameter d and polymer particles with diameter $2R_g$. The colloid-colloid and colloid-polymer interactions are considered to be hard-sphere-like, whereas polymer-polymer interactions are taken ideal. The presence of polymer induces a depletion attraction between the colloidal particles, which may ultimately lead to phase separation.[15–18] The resulting interface of the demixed colloid-polymer system is studied by Vink *et al.*[3] for a number of polymer concentrations and for a polymer-colloid size ratio parameter $\varepsilon \equiv 1 + 2R_g/d = 1.8$.

To study the interfacial fluctuations, Vink *et al.*[3] introduced the local interface position as

$$z_G(\vec{r}_\parallel) \equiv \frac{1}{\Delta\rho} \int_{-L}^{L} dz[\rho(\vec{r}) - \rho_{step}(z)], \tag{34}$$

where $\rho(\vec{r})$ can be taken to be either the colloid or polymer density. The integration limits $\pm L$ are inside the bulk regions, but different values for it are systematically considered.[3] One may easily verify that the correlations of the local interface position are exactly described by the surface structure factor defined earlier in Eq. (23),

$$\langle z_G(\vec{r}_{1,\parallel}) z_G(\vec{r}_{2,\parallel}) \rangle = S(r_\parallel). \tag{35}$$

In Fig. 2, typical results for the Fourier transform of the

surface structure obtained in the MC simulations of Vink *et al.*[3] are shown (Fig. 13 of Ref. [3]). In this example the integration limit is varied, $L/W = 1, 2, 3, 4$, where W is some measure of the interfacial thickness. One clearly observes that when L/W is too small, the results do not match the classical CW behavior for small q (dashed line), and that the contribution from bulklike fluctuations at high q increases with L/W.

In Fig. 3, we consider the result from Fig. 2 for $L/W = 3$. For small q the results asymptotically approach the result of the classical CW model (dotted line) with the value of σ taken from separate simulations. The dashed line is the combination of the CW model with the bulk correlation function

$$S(q) = \frac{k_B T}{\sigma q^2} + \mathcal{N}_L S_b(q). \tag{36}$$

The value of $\mathcal{N}_L$ is chosen such that it matches the $q \to \infty$ limit for $S(q)$ in Fig. 3. One finds that Eq. (36) already matches the simulation results quite accurately except at intermediate values of q, $qd \approx 1$.

As a next step, we investigate whether the inclusion of a bending rigidity is able to describe the simulation results at the following intermediate values:

$$S(q) = \frac{k_B T}{\sigma q^2 + k^{ic} q^4 + \cdots} + \mathcal{N}_L S_b(q). \tag{37}$$

The bending rigidity describes the leading order correction to the classical CW model in an expansion in q^2. Its value is therefore obtained from analyzing the behavior of $S(q)$ when $qd \lesssim 1$. The fact that the simulation results in Fig. 3 are systematically *above* the CW prediction in this region indicates that the bending rigidity thus obtained is *negative*, $k^{ic} < 0$. Unfortunately, a negative bending rigidity prohibits the use of Eq. (37) to fit the simulation results in the *entire* q-range since the denominator becomes zero at a certain value of q. It is therefore convenient to rewrite the expansion in q^2 in Eq. (37) in the following form:

TABLE I. Listed are the simulation results (Ref. 3) for the polymer volume fraction η_p, liquid and vapor colloidal volume fractions, η_ℓ and η_v, surface tension σ (in units of $k_B T/d^2$), bending rigidity k (in units of $k_B T$; in parentheses is the estimated error in the last digit), and $\sqrt{-k/\sigma}$ (in units of d).

η_p	η_ℓ	η_v	σ	k	$\sqrt{-k/\sigma}$
0.9	0.2970	0.0141	0.1532	−0.045(15)	0.40
1.0	0.3271	0.0062	0.2848	−0.07 (2)	0.50
1.1	0.3485	0.0030	0.4194	−0.10 (3)	0.49
1.2	0.3647	0.0018	0.5555	−0.14 (3)	0.50

$$S(q) = \frac{k_B T}{\sigma q^2}\left(1 - \frac{k^{ic}}{\sigma}q^2 + \cdots\right) + \mathcal{N}_L S_b(q), \tag{38}$$

which is equivalent to Eq. (37) to the order in q considered, but which has the advantage of being well behaved in the entire q-range. Other forms to regulate $S(q)$, which are equivalent to Eq. (37) to the order in q considered, may certainly be formulated. In analogy with a similar treatment of CWs by Parry *et al.*[27] in the context of wetting transitions, one might suggest that the appearance of a negative bending rigidity indicates the missing of a correlation length that would replace Eq. (38) with an explicit formula valid for all values of q, not just to the order in q considered.

The above form for $S(q)$ in Eq. (38), with the bending rigidity used as an adjustable parameter ($k=-0.045k_B T$), is plotted in Fig. 3 as the drawn line. Exceptionally good agreement with the MC simulations is obtained. In Table I, we list values of the bending rigidity obtained for a number of polymer volume fractions, η_p. These values are the results of fits of $S(q)$ from MC simulations for several system sizes and for several values of L/W, with the error estimated from the standard deviation of the various results. For the $L/W=1$ and $L/W=2$ curves (see Fig. 2), one needs to adjust for the fact that the CW limit is not correctly approached at low q. For the results in Fig. 2, one ultimately obtains for the bending rigidity $k=-0.040, -0.040, -0.045, -0.060k_B T$, for $L/W=1$, 2, 3, and 4, respectively.

In Table I, it should be reminded that, rather than the true polymer volume fraction in either phase, η_p should be interpreted as the polymer volume fraction of a reservoir fixing the polymer chemical potential.[28] Furthermore, the "liquid" is defined as the phase relatively rich in colloids and the "vapor" as the phase relatively poor in colloids.

The excellent agreement between Eq. (38) and the MC simulations is even more apparent in Fig. 4 where the results in Fig. 3 are redrawn on a linear scale. In Fig. 4 we also show the simulation results[3] and the corresponding fit using the *polymer particles* to define the location of the interface. As the polymer-polymer interactions are considered ideal, the bulk structure factor $S_b(q)=1$ in this case.

It is important to note that, effectively, the inclusion of a bending rigidity in the CW model results in the presence of an additive factor in $S(q)$ that is adjusted, see Eq. (38). The determination of the value for k^{ic} from the behavior of $S(q)$ near $q=0$, therefore, requires one to take into account the presence of the bulklike fluctuations since they *also* contribute as an additive constant, $\mathcal{N}_L S_b(0)$, near $q=0$. This means that even though the MC simulation results of Vink *et al.*[3] are very accurately described by Eq. (38), the resulting value

obtained for k^{ic} sensitively depends on the theoretical expression used for $S_b(0)$. Here we have simply approximated the bulk correlation function by the PY hard-sphere expression in the liquid,[26] but one could imagine more sophisticated expressions leading to a somewhat different value for k^{ic}.

In Secs. IV–VI we investigate whether the values for the bending rigidity obtained from the simulations (Table I) can also be described in the context of a molecular theory.

IV. DENSITY FUNCTIONAL THEORY

Our task in this section is straightforward. Using the expression for $\rho(\vec{r})$ given in Eq. (9), we determine $\Delta\Omega$ and the resulting $\sigma(q)$. To achieve this, we need a model for the free energy and define a procedure to determine the density profiles, $\rho_0(z)$ and $\rho_1(z)$, that are present in the expression for $\rho(\vec{r})$. We choose to perform these tasks in the context of DFT.

In the DFT for an inhomogeneous system that we consider,[5–7,19] the free energy is given by the free energy of the reference hard-sphere system augmented by an integral nonlocal term that considers the attractive part of the interaction potential, $U(r)=U_{hs}(r)+U_{att}(r)$,

$$\Omega[\rho] = \int d\vec{r}_1 g_{hs}(\rho) + \frac{1}{2}\int d\vec{r}_1 \int d\vec{r}_2 U_{att}(r)\rho(\vec{r}_1)\rho(\vec{r}_2). \tag{39}$$

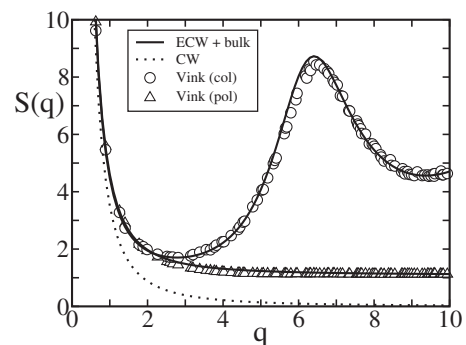For explicit calculations, $g_{hs}(\rho)$ is taken to be of the Carnahan–Starling form[29]

FIG. 4. MC results by Vink *et al.* (Ref. 3) for the surface structure factor (in units of d^4) vs q (in units of $1/d$) using the colloidal particles (circles) and polymer particles (triangles) to define z_G. The dotted line is the CW model and the drawn lines are the combination of the ECW model and the bulk correlation function. In this example, $\varepsilon=1.8$, $\eta_p=1.0$, and $L/W=3$.

$$g_{hs}(\rho) = k_B T \rho \ln(\rho) + k_B T \rho \frac{(4\eta - 3\eta^2)}{(1-\eta)^2} - \mu\rho, \qquad (40)$$

where $\eta \equiv (\pi/6)\rho d^3$. In the uniform bulk region, the free energy equals

$$\frac{\Omega(\rho)}{V} \equiv g(\rho) = g_{hs}(\rho) - a\rho^2, \qquad (41)$$

with the van der Waals parameter a given by[7]

$$a \equiv -\frac{1}{2}\int d\vec{r}_{12} U_{att}(r). \qquad (42)$$

The integration over $\vec{r}_{12}$ is restricted to the region $r > d$. This is not explicitly indicated; instead, we adhere to the convention that the attractive part of the interaction potential $U_{att}(r) = 0$ when $r < d$. The chemical potential μ is fixed by the condition of two-phase coexistence, $\mu = \mu_{coex}$, which implies that μ_{coex}, ρ_v, and ρ_ℓ are determined from the following set of equations: $g'(\rho_v) = 0$, $g'(\rho_\ell) = 0$, and $g(\rho_v) = g(\rho_\ell) = -p$.

To determine the change in free energy due to density fluctuations, we insert the expression for $\rho(\vec{r})$ given by Eq. (9) into the expression for Ω in Eq. (39). One then finds for $\Delta\Omega = \Omega - \sigma A$

$$\Delta\Omega = \frac{1}{8}\int d\vec{r}_1 \{g''_{hs}(\rho_0)\rho_1(z_1)^2[\Delta h(\vec{r}_{1,\parallel})]^2$$

$$+ \frac{1}{8}\int d\vec{r}_1 \int d\vec{r}_{12} U_{att}(r)\{-2\rho'_0(z_1)\rho'_0(z_2)[h(\vec{r}_{2,\parallel})$$

$$- h(\vec{r}_{1,\parallel})]^2 + 4\rho_1(z_1)\rho'_0(z_2)\Delta h(\vec{r}_{1,\parallel})[h(\vec{r}_{2,\parallel}) - h(\vec{r}_{1,\parallel})]$$

$$+ \rho_1(z_1)\rho_1(z_2)\Delta h(\vec{r}_{1,\parallel})\Delta h(\vec{r}_{2,\parallel})\}. \qquad (43)$$

Even though the derivation is somewhat different, this expression equals that given by Mecke and Dietrich[19] apart from a gravity term that was included in their expression. To cast $\Delta\Omega$ in the form of Eq. (11), we take the Fourier transform. One then finds for $\sigma(q)$ (Ref. 19)

$$\sigma(q) = \int_{-\infty}^{\infty} dz_1 \int_{-\infty}^{\infty} dz_{12} \left[\frac{\omega(q,z_{12}) - \omega_0(z_{12})}{q^2}\right]$$

$$\times [\rho'_0(z_1)\rho'_0(z_2) - q^2\rho_1(z_1)\rho'_0(z_2)]$$

$$+ \frac{q^2}{4}\int_{-\infty}^{\infty} dz_1 \int_{-\infty}^{\infty} dz_{12}\omega(q,z_{12})\rho_1(z_1)\rho_1(z_2)$$

$$+ \frac{q^2}{4}\int_{-\infty}^{\infty} dz_1 g''_{hs}(\rho_0)\rho_1(z_1)^2. \qquad (44)$$

Here we have defined the (parallel) Fourier transform of the interaction potential

$$\omega(q,z_{12}) \equiv \int d\vec{r}_\parallel e^{-i\vec{q}\cdot\vec{r}_\parallel} U_{att}(r) = 2\pi\int_0^\infty dr_\parallel r_\parallel J_0(qr_\parallel)U_{att}(r). \qquad (45)$$

As a first step, we determine the leading contribution to $\sigma(q)$ given by the surface tension of the *planar* interface, $\sigma = \sigma(q=0)$. Then, one needs to consider the two leading contributions in the expansion of $\omega(q,z_{12})$ in q^2 as follows:

$$\omega(q,z_{12}) = \omega_0(z_{12}) + \omega_2(z_{12})q^2 + \cdots, \qquad (46)$$

where

$$\omega_0(z_{12}) \equiv \int d\vec{r}_\parallel U_{att}(r),$$

$$\omega_2(z_{12}) \equiv -\frac{1}{4}\int d\vec{r}_\parallel r_\parallel^2 U_{att}(r). \qquad (47)$$

The surface tension thus becomes

$$\sigma = \int_{-\infty}^{\infty} dz_1 \int_{-\infty}^{\infty} dz_{12}\omega_2(z_{12})\rho'_0(z_1)\rho'_0(z_2). \qquad (48)$$

The (planar) density profile $\rho_0(z)$, featured in the above expression for σ, is determined from minimizing the free energy functional $\Omega[\rho]$ in Eq. (39) in planar symmetry. The Euler–Lagrange equation that minimizes $\Omega[\rho]$ is then given by

$$g'_{hs}(\rho_0) = -\int d\vec{r}_{12} U_{att}(r)\rho_0(z_2) = -\int_{-\infty}^{\infty} dz_{12}\omega_0(z_{12})\rho_0(z_2), \qquad (49)$$

which can be solved explicitly to obtain $\rho_0(z)$ and thus σ.

The evaluation of further contributions to $\sigma(q)$ requires one to determine the density profile $\rho_1(z)$. Just like $\rho_0(z)$, one would like to determine the density profile $\rho_1(z)$ from a minimization procedure. One then has to determine the energetically most favorable density profile for a *given* curvature of the surface.[21] This turns out to be not so straightforward, since one then has to specify in what way the curvature is set to its given value. Several approaches have been suggested, which we shall now discuss.

- *Mecke and Dietrich approach.* In this approach a certain form for $\rho_1(z)$ is directly hypothesized,[19]

$$\rho_1^{MD}(z) = -\frac{C_H}{2\pi}\Delta\rho\xi f_H(z/\xi), \qquad (50)$$

with ξ the bulk correlation length and $f_H(x) \equiv x \sinh(x/2)/\cosh^2(x/2)$. The coefficient C_H in this expression can be used as a fit parameter. This practical approach is certainly legitimate, but one would like to also be able to formulate a molecular basis for this expression.

- *Equilibrium approach.* Rather than the surface being curved by surface fluctuations, in this approach the interface is curved by changing the value of the chemical potential to a value *off coexistence*. One then considers the density profile of a spherically or cylindrically shaped liquid droplet in metastable equilibrium with a bulk vapor.[20,25] This approach is equivalent to adding an external field to the free energy

$$\Omega'[\rho] = \Omega[\rho] + \int d\vec{r} V_{\text{ext}}(\vec{r})\rho(\vec{r}) = \Omega[\rho] - \int d\vec{r}\Delta\mu\rho(\vec{r}),$$

$$(51)$$

where $\Delta\mu = \mu - \mu_{\text{coex}}$. The downside of the equilibrium approach is that the external field $V_{\text{ext}}(\vec{r}) = -\Delta\mu$ is uniform throughout the system and thus also affects the bulk densities far from the interfacial region. This seems inappropriate for the description of the density fluctuations considered here since we have that $\mu = \mu_{\text{coex}}$ and the bulk densities are unaltered by the curvature of the surface fluctuations.

- *Local external field.* In this approach, one again adds to the free energy an external field, but, to ensure that the bulk regions are unaffected, one assumes that it is peaked infinitely sharply at $z=0$ as follows:[21,22]

$$V_{\text{ext}}(\vec{r}) = \lambda\,\delta(z)\Delta h(\vec{r}_\parallel).$$

$$(52)$$

In this case, the external field only acts as a Lagrange multiplier in the minimization procedure to ensure that the curvature $\Delta h(\vec{r}_\parallel)$ is set to a certain value; it is not included in the expression for the free energy. The downside of this method is that the resulting density profile $\rho_1(z)$ has a discontinuous first derivative at $z=0$, which is, from a physical point of view, not so appealing.[30] Furthermore, the discontinuous nature of $\rho_1(z)$ prohibits an analytical simplification using a gradient expansion.

In the present approach, we suggest to add an external field acting as a Lagrange multiplier that is unequal to zero only in the interfacial region (the bulk densities are unaffected), but which is not infinitely sharp peaked. It seems natural to choose a peak width of the order of the thickness of the interfacial region. It thus seems convenient to choose $V_{\text{ext}}(\vec{r}) \propto \rho_0'(z)$ as follows:

$$V_{\text{ext}}(\vec{r}) = \lambda\rho_0'(z)\Delta h(\vec{r}_\parallel).$$

$$(53)$$

This choice for $V_{\text{ext}}(\vec{r})$ constitutes our fundamental "ansatz" for the determination of $\rho_1(z)$. The Lagrange multiplier λ is not a free parameter but set by the imposed curvature, as demonstrated below.

The addition of an external field to the free energy results in the following Euler–Lagrange equation:

$$g_{\text{hs}}'(\rho) = -\int d\vec{r}_{12} U_{\text{att}}(r)\rho(\vec{r}_2) - V_{\text{ext}}(\vec{r}).$$

$$(54)$$

Using the external field given in Eq. (53), we insert the fluctuating density given by Eq. (9) into the above Euler–Lagrange equation. In order for the resulting equation to hold independently of the value of $h(\vec{r}_\parallel)$ or $\Delta h(\vec{r}_\parallel)$, one finds, besides Eq. (49), the following equation to determine $\rho_1(z)$:

$$g_{\text{hs}}''(\rho_0)\rho_1(z_1) = -\int_{-\infty}^{\infty} dz_{12}\omega_0(z_{12})\rho_1(z_2)$$

$$+ 2\int_{-\infty}^{\infty} dz_{12}\omega_2(z_{12})\rho_0'(z_2) + 2\lambda\rho_0'(z_1).$$

$$(55)$$

The value of the Lagrange multiplier can be determined by multiplying both sides of the above expression by $\rho_0'(z_1)$ and integrating over z_1 as follows:

$$\lambda = -\sigma \left/ \left[\int dz [\rho_0'(z)]^2 \right] \right.$$

$$(56)$$

One may now verify that if $\rho_1(z)$ is a particular solution of Eq. (55) then $\rho_1(z) + \alpha\rho_0'(z)$ is a solution on account of Eq. (49).

It is convenient to use the Euler–Lagrange equation in Eq. (55) to remove the explicit appearance of $g_{\text{hs}}''(\rho_0)$ in the expression for $\sigma(q)$ in Eq. (44). The resulting $\sigma(q)$ is written as the sum of a term that depends only on the density profile $\rho_0(z)$ and one term that also depends on the density profile $\rho_1(z)$ as follows:

$$\sigma(q) = \sigma_0(q) + k_1 q^2 + \mathcal{O}(q^4),$$

$$(57)$$

with

$$\sigma_0(q) \equiv \int_{-\infty}^{\infty} dz_1 \int_{-\infty}^{\infty} dz_{12} \left[\frac{\omega(q,z_{12}) - \omega_0(z_{12})}{q^2} \right] \rho_0'(z_1)\rho_0'(z_2),$$

$$k_1 \equiv -\frac{1}{2}\int_{-\infty}^{\infty} dz_1 \int_{-\infty}^{\infty} dz_{12}\omega_2(z_{12})\rho_1(z_1)\rho_0'(z_2)$$

$$+ \frac{\lambda}{2}\int_{-\infty}^{\infty} dz_1\rho_1(z_1)\rho_0'(z_1).$$

$$(58)$$

With the above expression for k_1 it is now also possible to verify that when the density profile $\rho_1(z)$ is shifted by a factor $\alpha\rho_0'(z)$, the resulting effect on the bending parameters is that given by Eq. (22).

The procedure to determine $\sigma(q)$, and therefore σ, k, k_s, and ℓ_k, is now as follows: Assuming a certain form for the attractive part of the interaction potential, $\rho_0(z)$ is obtained from solving Eq. (49), which is then inserted into Eq. (55) to solve for $\rho_1(z)$ explicitly. The two density profiles thus obtained are inserted into Eq. (58) to yield $\sigma_0(q)$ and k_1. This procedure is carried out in Secs. V and VI considering SR forces and LR forces $(U(r) \propto 1/r^6)$. In general the density profiles $\rho_0(z)$ and $\rho_1(z)$ need to be determined numerically. We shall, however, also provide an approximation scheme, based on the gradient expansion, that is exact near the critical point, but which also gives an excellent approximation far from it.

A. Gradient expansion

The gradient approximation[7] is based on the assumption that the spatial variation of the density profile is small, i.e.,

$$\rho(z_2) = \rho(z_1) + z_{12}\rho'(z_1) + \frac{z_{12}^2}{2}\rho''(z_1) + \cdots. \tag{59}$$

In the gradient expansion, the Euler–Lagrange equation in Eq. (49) for $\rho_0(z)$ reduces to

$$g'(\rho_0) = 2m\rho_0''(z), \tag{60}$$

where m is the van der Waals squared-gradient coefficient[7]

$$m \equiv -\frac{1}{12}\int d\vec{r}_{12} r^2 U_{\text{att}}(r) = \frac{1}{2}\int_{-\infty}^{\infty} dz_{12}\omega_2(z_{12})$$

$$= \frac{1}{4}\int_{-\infty}^{\infty} dz_{12}z_{12}^2\omega_0(z_{12}). \tag{61}$$

In the gradient expansion, the Euler–Lagrange equation in Eq. (55) for $\rho_1(z)$ reduces to

$$m\frac{\rho_0'''(z_1)}{\rho_0'(z_1)}\rho_1(z_1) = m\rho_1''(z_1) + \int_{-\infty}^{\infty} dz_{12}\omega_2(z_{12})\rho_0'(z_2)$$

$$+ \lambda\rho_0'(z_1), \tag{62}$$

where we have used Eq. (60) to replace $g_{\text{hs}}''(\rho_0)$.

First, we consider the determination of the density profile $\rho_0(z)$. The gradient expansion becomes exact near the critical point where $g(\rho)$ takes on the usual double-well form

$$g(\rho) + p = \frac{m}{(\Delta\rho)^2\xi^2}(\rho - \rho_\ell)^2(\rho - \rho_v)^2. \tag{63}$$

Using this form for $g(\rho)$, the solution of the Euler–Lagrange equation in Eq. (60) gives the usual tanh-form for $\rho_0(z)$ as follows:[7]

$$\rho_0(z) = \frac{1}{2}(\rho_\ell + \rho_v) - \frac{\Delta\rho}{2}\tanh(z/2\xi), \tag{64}$$

with the bulk correlation length ξ a measure of the interfacial thickness.

Even though the tanh-form for the density profile $\rho_0(z)$ is derived assuming proximity to the critical point, it turns out that it also provides a good approximation away from it when one determines the value of ξ by fitting the surface tension to its form near the critical point. In the squared-gradient approximation, Eq. (48) reduces to the familiar expression[7]

$$\sigma = 2m\int_{-\infty}^{\infty} dz\rho_0'(z)^2 = 2\sqrt{m}\int_{\rho_v}^{\rho_\ell} d\rho\sqrt{g(\rho) + p}. \tag{65}$$

On the one hand, the surface tension can be determined from the above approximation using the full form for $g(\rho)$ given in Eqs. (40) and (41),

$$\sigma = 2\sqrt{m}\int_{\rho_v}^{\rho_\ell} d\rho\left[k_BT\rho\ln(\rho) + k_BT\rho\frac{(4\eta - 3\eta^2)}{(1 - \eta)^2}\right.$$

$$\left. - \mu_{\text{coex}}\rho - a\rho^2 + p\right]^{1/2}. \tag{66}$$

On the other hand, near the critical point, $g(\rho)$ takes on the double-well form in Eq. (63) and σ is calculated as
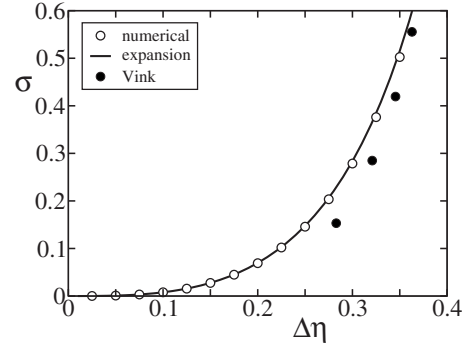

FIG. 5. Surface tension in units of k_BT/d^2 vs the volume fraction difference, $\Delta\eta$. In this example, $\varepsilon = 1.8$; the symbols are numerical results, the drawn line is the gradient expansion approximation, and the filled symbols are results from the MC simulations by Vink et al. (Ref. 3).

$$\sigma = \frac{m(\Delta\rho)^2}{3\xi}. \tag{67}$$

Now, we define the value of ξ such that the two expressions for the surface tension in Eqs. (66) and (67) are equal. This gives for ξ

$$\xi \equiv \frac{m(\Delta\rho)^2}{3\sigma}, \tag{68}$$

with σ given by Eq. (66).

Next, we turn to the evaluation of $\rho_1(z)$ from Eq. (62). This requires one to make a distinction between SR forces and LR forces.

V. DFT: SHORT-RANGED INTERACTIONS

Although the analysis below is quite generally valid for all SR interaction potentials, whenever we show explicit results, we consider for $U_{\text{att}}(r)$ the Asakura–Oosawa–Vrij depletion interaction potential $U_{\text{dep}}(r)$ as an example,[15]

$$U_{\text{dep}}(r) = \frac{-k_BT\eta_p}{2(\varepsilon - 1)^3}\left[2\varepsilon^3 - 3\varepsilon^2\left(\frac{r}{d}\right) + \left(\frac{r}{d}\right)^3\right], \tag{69}$$

where the intermolecular distance is in the range $1 < r/d < \varepsilon$. Interaction parameters based on the depletion potential are listed in Appendix A. The strength of the depletion interaction potential as determined by the polymer volume fraction η_p determines the location in the phase diagram;[16,28] for comparison with other results, it is, however, more convenient to use the colloidal density difference $\Delta\eta \equiv \eta_\ell - \eta_v$ as a thermodynamic variable.[31]

In Fig. 5, the surface tension is shown as a function of $\Delta\eta$. The open circles are obtained from numerically solving the Euler–Lagrange equation in Eq. (49) for $\rho_0(z)$ and inserting the result into Eq. (48). The drawn line is the gradient expansion approximation for σ in Eq. (66). Also shown are the results from the MC simulations by Vink et al.[3] The gradient expansion gives a very good approximation to the numerical results and is in good agreement with the simulations.

For SR forces the expansion in q^2 of the expression for $\omega(q, z_{12})$ as defined by Eq. (45) can be continued to $\mathcal{O}(q^4)$ as follows:

$$\omega(q, z_{12}) = \omega_0(z_{12}) + \omega_2(z_{12})q^2 + \omega_4(z_{12})q^4 + \cdots, \quad (70)$$

where

$$\omega_4(z_{12}) \equiv \frac{1}{64} \int d\vec{r}_\| r_\|^4 U_{att}(r). \quad (71)$$

With this expansion, $\sigma(q)$ in Eq. (58) can now be written in the form of Eq. (13)

$$\sigma(q) = \sigma + kq^2 + \mathcal{O}(q^4) = \sigma + k_0 q^2 + k_1 q^2 + \mathcal{O}(q^4), \quad (72)$$

with the bending rigidity $k = k_0 + k_1$ and

$$k_0 = \int_{-\infty}^{\infty} dz_1 \int_{-\infty}^{\infty} dz_{12} \omega_4(z_{12}) \rho_0'(z_1) \rho_0'(z_2), \quad (73)$$

$$k_1 = -\frac{1}{2} \int_{-\infty}^{\infty} dz_1 \int_{-\infty}^{\infty} dz_{12} \omega_2(z_{12}) \rho_1(z_1) \rho_0'(z_2)$$
$$+ \frac{\lambda}{2} \int_{-\infty}^{\infty} dz_1 \rho_1(z_1) \rho_0'(z_1).$$

Next, we proceed to evaluate these expressions in the gradient expansion.

A. Gradient expansion for short-ranged forces

In the gradient expansion, k_0 and k_1 in Eq. (73) reduce to

$$k_0 = -\frac{B}{2} \int_{-\infty}^{\infty} dz \rho_0'(z)^2, \quad (74)$$

$$k_1 = -2m \int_{-\infty}^{\infty} dz \rho_1(z) \rho_0'(z),$$

where we have used the fact that to leading order in the gradient expansion $\lambda \approx -2m$, and where we have defined[32]

$$B \equiv -\frac{1}{60} \int d\vec{r}_{12} r^4 U_{att}(r) = -2 \int_{-\infty}^{\infty} dz_{12} \omega_4(z_{12})$$
$$= \frac{1}{2} \int_{-\infty}^{\infty} dz_{12} z_{12}^2 \omega_2(z_{12}). \quad (75)$$

Inserting the tanh-form for $\rho_0(z)$ into Eq. (74), one directly obtains for k_0

$$k_0 = -\frac{B(\Delta\rho)^2}{12\xi} = -\frac{B\sigma}{4m}, \quad (76)$$

where we have used the expression for ξ in Eq. (68) to rewrite k_0 as the latter expression.

To evaluate k_1 in Eq. (74), we need to determine $\rho_1(z)$ from the Euler–Lagrange equation in Eq. (62). For SR forces, Eq. (62) reduces to

$$m \frac{\rho_0'''(z)}{\rho_0'(z)} \rho_1(z) = m \rho_1''(z) + B \rho_0'''(z) + \beta B \rho_0'(z), \quad (77)$$
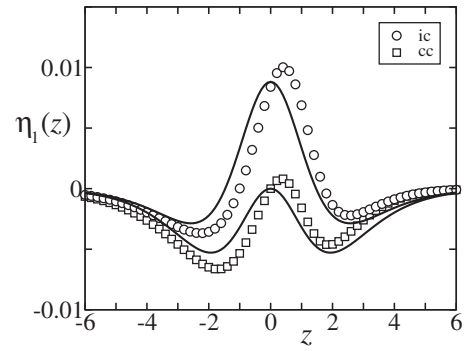
where we have defined

FIG. 6. Curvature correction to the volume fraction profile $\eta_1(z)$ as a function of z (in units of d) using the ic (circles) and the cc (squares). In this example, $\Delta\eta = 0.25$ and $\varepsilon = 1.8$; the symbols are numerical results and the drawn lines are the analytical profiles from the gradient expansion.

$$\beta \equiv \frac{\int dz \rho_0''(z)^2}{\int dz \rho_0'(z)^2}. \quad (78)$$

Using the tanh-profile for $\rho_0(z)$ in Eq. (64), one has $\beta = 1/(5\xi^2)$ and finds for $\rho_1(z)$ from solving the differential equation in Eq. (77)

$$\rho_1^{cc}(z) = -\frac{3B}{10m} \frac{\Delta\rho}{\xi} \frac{\ln(\cosh(z/2\xi))}{\cosh^2(z/2\xi)}. \quad (79)$$

The above profile corresponds to that obtained using the cc. The profile corresponding to the ic follows from $\rho_1^{ic} = \rho_1^{cc} + \alpha \rho_0'$ [Eq. (20)], with α determined by Eq. (21). This gives

$$\rho_1^{ic}(z) = \frac{3B}{10m} \frac{\Delta\rho}{\xi} \frac{[1 - \ln(2 \cosh(z/2\xi))]}{\cosh^2(z/2\xi)}. \quad (80)$$

In Fig. 6, typical volume fraction profiles $\eta_1(z) = (\pi/6)d^3 \rho_1(z)$ are shown for the cc and the ic. The symbols are the profiles obtained from numerically solving the Euler–Lagrange equation in Eq. (55), whereas the drawn lines are the approximate profiles in Eqs. (79) and (80) obtained from the gradient expansion.

Inserting the density profiles $\rho_1^{ic}(z)$ and $\rho_1^{cc}(z)$ into the expression for k_1 in Eq. (74), one obtains

$$k_1^{cc} = -\frac{B(\Delta\rho)^2}{\xi} \left[\frac{1}{3} - \frac{2}{5}\ln(2) \right] = -\frac{B\sigma}{m} \left[1 - \frac{6}{5}\ln(2) \right],$$
$$k_1^{ic} = \frac{B(\Delta\rho)^2}{15\xi} = \frac{B\sigma}{5m}. \quad (81)$$

In Fig. 7, k_0, k_1^{ic}, and k_1^{cc} are shown as a function of $\Delta\eta$. The open symbols are obtained from numerically solving Eqs. (49) and (55) to obtain $\rho_0(z)$ and $\rho_1(z)$ and inserting the result into Eq. (73). The drawn lines are the gradient expansion approximation for k_0 in Eq. (76) and k_1 in Eq. (81). Adding the results for k_1 in Eq. (81) to k_0 in Eq. (76), one obtains for the bending rigidities

$$k^{cc} = -\frac{B(\Delta\rho)^2}{\xi} \left[\frac{5}{12} - \frac{2}{5}\ln(2) \right] = -\frac{B\sigma}{m} \left[\frac{5}{4} - \frac{6}{5}\ln(2) \right],$$
$$(82)$$

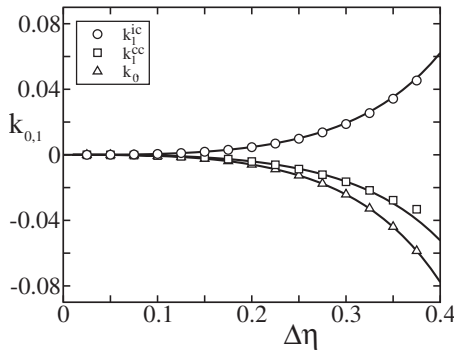$$k^{ic} = -\frac{B(\Delta\rho)^2}{60\xi} = -\frac{B\sigma}{20m}.$$

FIG. 7. Contributions to the bending rigidity k_0 and k_1 in units of k_BT vs the volume fraction difference, $\Delta\eta$. In this example, $\varepsilon = 1.8$; the symbols are numerical results and the drawn lines are the gradient expansion approximation.

In Fig. 8, the bending rigidity is shown as a function of $\Delta\eta$. The open symbols are the numerical results. The drawn lines are the gradient expansion approximations in Eq. (82), $\sqrt{-k^{cc}/\sigma} \approx 0.378d$ and $\sqrt{-k^{ic}/\sigma} \approx 0.131d$.

The resulting values for both bending rigidities, k^{cc} and k^{ic}, are negative in line with the simulation results of Vink *et al.*[3] (filled circles). However, the value of k^{ic}, which is the relevant value when we compare with the simulations, is significantly less negative. As stressed earlier, the bending rigidity depends on the constraint used to define the height profile $h(\vec{r}_\parallel)$ through the contribution to k coming from k_1. We demonstrated that in the cc k_1^{cc} is negative whereas in the ic k_1^{ic} is positive. One could very well imagine that a different constraint used to determine the height profile $h(\vec{r}_\parallel)$ might lead to a bending rigidity that is positive.[4] For the ic the two contributions to k from k_0 and k_1^{ic} nearly cancel leading to a value for k^{ic}, which is barely negative. Unfortunately, this makes the value of k^{ic} sensitively dependent on the precise model used to determine $\rho_1(z)$.

An important point concerns the *scaling behavior* of the bending rigidity. The expressions in Eq. (82) indicate that the bending rigidity vanishes near the critical point with the same exponent as the surface tension, i.e.,
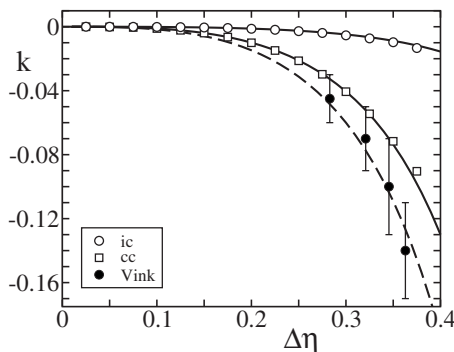

FIG. 8. Bending rigidity in units of k_BT vs the volume fraction difference, $\Delta\eta$, using the ic (circles) and the cc (squares). In this example, $\varepsilon = 1.8$; the open symbols are numerical results, the drawn lines are the gradient expansion approximation, and the filled circles are the MC results by Vink *et al.* (Ref. 3); the dashed line is the fit $\sqrt{-k/\sigma} \approx 0.47d$.

$$k \propto \frac{B\sigma}{m} \propto \sigma d^2. \tag{83}$$

Note that for the depletion potential, the ratio B/m only depends on the size ratio parameter ε ($B/m \approx 0.342d^2$ for $\varepsilon = 1.8$) but is independent of η_p (or $\Delta\eta$); see Appendix A. Both contributions to the bending rigidity, k_0 and k_1, show the above scaling behavior and both should therefore be taken into account.

The scaling result in Eq. (83) should be contrasted with the usual assumption that $k \propto \sigma\xi^2$, i.e., the bending rigidity approaches a finite, nonzero limit at the critical point. This scaling behavior is, for instance, obtained for the bending rigidity k_{eq} determined from analyzing the surface tension of a spherically or cylindrically shaped liquid droplet in metastable equilibrium with a bulk vapor.[20,25] In the gradient expansion, one has[20]

$$k_{eq} = -\frac{1}{9}(\pi^2 - 3)m(\Delta\rho)^2\xi. \tag{84}$$

It is perhaps important to discuss more broadly this result in the context of previous work on the virial approach[24] to the bending rigidity (and other curvature parameters). The virial expression for the bending rigidity is generally valid, but it is important to realize that it features the way in which the pair density depends on curvature.[24] When a mean-field, squared-gradient approximation is subsequently made,[20] this translates into the expression for the bending rigidity to depend on the way in which the *density* depends on curvature, i.e., it features the profile $\rho_1(z)$. Therefore, even though the expressions for the bending rigidity in the equilibrium approach and the fluctuating interface approach are the same, they might lead to different values (and scaling behavior) of the bending rigidity due to the fact that the density profiles $\rho_1(z)$ are different in these two cases.

It is interesting to also compare with the approach by Mecke and Dietrich.[19] Even though the goal in Ref. 19 is to consider LR forces, one may use the expression in Eq. (50) for $\rho_1^{MD}(z)$ inserted into Eq. (43) to determine the leading correction to $\sigma(q)$ also for SR forces. The gradient expansion then gives

$$k_{MD} = -\left[\frac{C_H}{6} - \frac{C_H^2}{24\pi^2}(\pi^2 + 16)\right]m(\Delta\rho)^2\xi. \tag{85}$$

The prefactor is negative (as long as $0 < C_H < 1.526$) in line with the results obtained here. Again, the scaling behavior—equal to that of k_{eq}—is essentially different from our prediction in Eq. (83).

Finally, we like to mention an expression for the bending rigidity that is derived from the generally valid virial expression,[24] in which the assumption is made that the width of the interfacial profile is much smaller than the molecular diameter $d \gg \xi$.[24,33] The implication is that $\rho_0(z) = \rho_{step}(z)$, the sharp-profile approximation, and $\rho_1(z) = 0$. The sharp-profile expressions for the surface tension (also known as the Fowler formula[34]) and bending rigidity are[22,24,34]
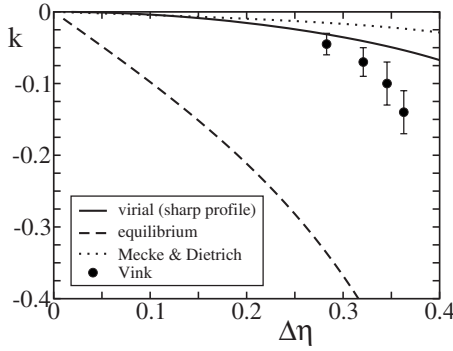
FIG. 9. Bending rigidity in units of k_BT vs the volume fraction difference, $\Delta\eta$. In this example, $\varepsilon=1.8$; the filled circles are the MC results by Vink *et al.* (Ref. 3), the drawn line is the virial expression with the sharp-profile approximation, the dashed line is the equilibrium result, and the dotted line is the Mecke and Dietrich result (Ref. 19) with $C_H=1/4$.

$$\sigma_{sp} = \frac{(\Delta\rho)^2}{32} \int d\vec{r}_{12} r^2 U'(r) g_\ell(r),$$

$$k_{sp} = -\frac{(\Delta\rho)^2}{768} \int d\vec{r}_{12} r^4 U'(r) g_\ell(r), \tag{86}$$

where $U(r)$ is the *full* interaction potential. Since $\rho_1(z)=0$, the expression for k_{sp} is independent of the constraint used to determine $\rho_1(z)$.

In Fig. 9, the different models for the bending rigidity are compared to the simulation results of Vink *et al.*[3] For the evaluation of k_{sp} we have taken $g_\ell(r)=g_{hs}^{PY}(r;\eta_\ell)$.

VI. DFT: LONG-RANGED INTERACTIONS

Here we examine the case that the expansion of $\omega(q,z_{12})$ in q^2 *cannot* be continued to $\mathcal{O}(q^4)$. This is the case when the interaction potential falls of as $1/r^n$ at large distances, with $n \leq 6$. In particular, we shall assume the asymptotic behavior of $U_{att}(r)$ to be given by

$$U_{att}(r) = -A/r^6 \quad \text{when} \quad r \gg d. \tag{87}$$

The analysis below only assumes that the asymptotic behavior of $U_{att}(r)$ is given by the above expression. However, when we show explicit results, we consider the above form for $U_{att}(r)$ extended to the whole range $1 < r/d < \infty$ (see also Appendix B).

With the asymptotic behavior of $U_{att}(r)$ given by Eq. (87), the expansion of $\omega(q,z_{12})$ in q^2 takes on the form

$$\omega(q,z_{12}) = \omega_0(z_{12}) + \omega_2(z_{12})q^2 + \frac{\pi}{32}Aq^4 \ln(qd)$$

$$+ \omega_4(z_{12})q^4 + \cdots. \tag{88}$$

The coefficient of the $q^4 \ln(q)$-term only depends on the asymptotic behavior of the interaction potential as defined by the coefficient A, whereas $\omega_4(z_{12})$ depends on the interaction potential's full shape. With the expansion in Eq. (88), $\sigma(q)$ in Eq. (58) can now be written in the form of Eq. (15),[19]

$$\sigma(q) = \sigma + k_s q^2 \ln(qd) + k_0 q^2 + k_1 q^2 + \mathcal{O}(q^4)$$

$$\equiv \sigma + k_s q^2 \ln(q\ell_k) + \mathcal{O}(q^4) \tag{89}$$

with $k_s \ln(\ell_k/d) = k_0 + k_1$ and

$$k_s = \frac{\pi}{32}A(\Delta\rho)^2, \tag{90}$$

$$k_0 = \int_{-\infty}^\infty dz_1 \int_{-\infty}^\infty dz_{12}\omega_4(z_{12})\rho_0'(z_1)\rho_0'(z_2), \tag{91}$$

$$k_1 = -\frac{1}{2}\int_{-\infty}^\infty dz_1 \int_{-\infty}^\infty dz_{12}\omega_2(z_{12})\rho_1(z_1)\rho_0'(z_2)$$

$$+ \frac{\lambda}{2}\int_{-\infty}^\infty dz_1\rho_1(z_1)\rho_0'(z_1). \tag{92}$$

Next, we proceed to evaluate these expressions in the gradient expansion.

A. Gradient expansion for long-ranged forces

We first turn to the evaluation of k_0 in Eq. (91). A straightforward gradient expansion of $\rho_0'(z_2)$ is now not possible due to the fact that the integral $\int dz_{12}\omega_4(z_{12})$ is no longer finite.[19] The assumption of proximity to the critical point, however, does allow one to consider only the asymptotic form of $\omega_4(z_{12})$ at large distances. Using Eq. (87), one finds for $\omega_4(z_{12})$ as defined by Eq. (88)

$$\omega_4(z_{12}) = \frac{\pi A}{32}\left[\gamma_E - \frac{3}{4} + \frac{1}{2}\ln\left(\frac{z_{12}^2}{4d^2}\right)\right] + \mathcal{O}\left(\frac{d^2}{z_{12}^2}\right). \tag{93}$$

One now proceeds by inserting the above expression for $\omega_4(z_{12})$, together with the tanh-profile for $\rho_0(z)$ in Eq. (64), into the expression for k_0 in Eq. (91) and carrying out the remaining integrations over z_1 and z_{12}. One finds for k_0

$$k_0 = \frac{\pi}{32}A(\Delta\rho)^2\left[\ln(\xi/d) + c_0 + \mathcal{O}\left(\frac{d}{\xi}\right)\right], \tag{94}$$

where

$$c_0 = \gamma_E - \frac{3}{4} - \int_0^\infty dt \ln(t^2)\left[\frac{\sinh(t) - t\cosh(t)}{\sinh^3(t)}\right]$$

$$\approx -0.605\,270, \ldots . \tag{95}$$

Next, we turn to the evaluation of k_1. In the gradient expansion, the expression for k_1 in Eq. (92) reduces to

$$k_1 = -2m\int_{-\infty}^\infty dz\rho_1(z)\rho_0'(z). \tag{96}$$

The further evaluation of k_1 requires one to solve the Euler–Lagrange equation in Eq. (62) for $\rho_1(z)$. Again, a gradient expansion of $\rho_0'(z_2)$ is not possible due to the fact that now the integral $\int dz_{12}z_{12}^2\omega_2(z_{12})$ is no longer finite. Using the expression for the interaction potential in Eq. (87), one finds for $\omega_2(z_{12})$ when $|z_{12}| \gg d$
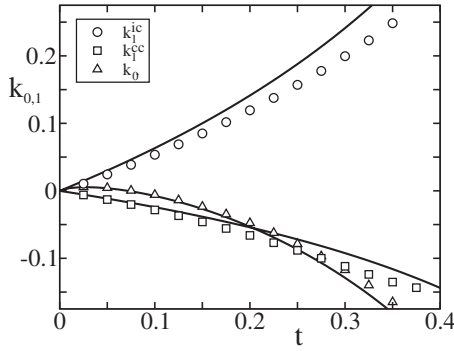
FIG. 10. Contributions to the bending rigidity k_0 and k_1 in units of $k_B T$ vs the reduced temperature distance to the critical point, t. The symbols are numerical results and the drawn lines are the gradient expansion approximation.

FIG. 11. The bending length ℓ_k (in units of d) vs the reduced temperature distance to the critical point, t, using the ic (circles) and the cc (squares). The open symbols are numerical results and the drawn lines are the gradient expansion approximation. The dashed line is the correlation length ξ and the dotted line is the Mecke and Dietrich result (Ref. 19) with $C_H = 1/4$.

$$\omega_2(z_{12}) = \frac{\pi A}{8 z_{12}^2} + \mathcal{O}\left(\frac{d^4}{z_{12}^4}\right). \tag{97}$$

The above expression for $\omega_2(z_{12})$ is used to solve Eq. (62) for $\rho_1(z)$, which is then inserted into the expression for k_1 in Eq. (96). After some algebra, one finally obtains for k_1

$$k_1^{cc} = \frac{\pi}{32} A (\Delta\rho)^2 \left[c_1^{cc} + \mathcal{O}\left(\frac{d}{\xi}\right) \right],$$

$$k_1^{ic} = \frac{\pi}{32} A (\Delta\rho)^2 \left[c_1^{ic} + \mathcal{O}\left(\frac{d}{\xi}\right) \right]. \tag{98}$$

with

$$c_1^{cc} \approx -0.559\,665, \ldots,$$

$$c_1^{ic} = \frac{4}{3} \int_0^\infty dt \ln(t) \left[\frac{\sinh^3(t) + 3\,\sinh(t) - 3t\,\cosh(t)}{t^2 \sinh^3(t)} \right]$$

$$\approx 1.461\,525, \ldots. \tag{99}$$

In Fig. 10, k_0, k_1^{ic}, and k_1^{cc} are shown as a function of the reduced temperature distance to the critical point, $t \equiv |1 - T/T_c|$. The open symbols are obtained from numerically solving Eqs. (49) and (55) to obtain $\rho_0(z)$ and $\rho_1(z)$ and inserting the result into Eqs. (91) and (92). The drawn lines are the gradient expansion approximation for k_0 in Eq. (94) and k_1 in Eq. (98).

Adding the expressions for k_0 in Eq. (94) and k_1 in Eq. (98), one obtains for ℓ_k

$$\ell_k^{cc} = \exp(c_0 + c_1^{cc}) \xi + \mathcal{O}(d) \approx 0.311\,942 \cdots \xi + \mathcal{O}(d),$$

$$\ell_k^{ic} = \exp(c_0 + c_1^{ic}) \xi + \mathcal{O}(d) \approx 2.354\,329 \cdots \xi + \mathcal{O}(d). \tag{100}$$

In Fig. 11, the bending length is shown as a function of t. The open symbols are the numerical results. The drawn lines are the gradient expansion approximations in Eq. (100).

Other than that the gradient expansion seems not to be as accurate in reproducing numerical results, the results in Figs. 10 and 11 are in line with the earlier results obtained for SR forces. The leading order correction to the surface tension is negative when $q\ell_k < 1$, and the effect is more pronounced for the cc than the ic. Although the goal of Mecke and Dietrich
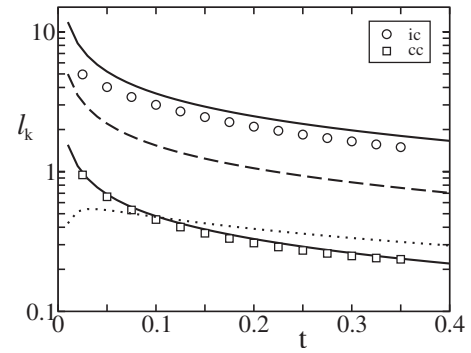
in Ref. 19 is to include higher order terms, terms beyond q^2 in the expansion of $\sigma(q)$, it is also interesting to compare with the Mecke and Dietrich[19] approach for the terms obtained to order $q^2 \ln(q)$ and q^2. Using the Mecke and Dietrich[19] expression for $\rho_1(z)$ in Eq. (50), one has to leading order in the gradient expansion

$$\sigma_{MD}(q) = \sigma + k_s q^2 \ln(qd) + k_0 q^2 + k_{MD} q^2 + \mathcal{O}(q^4)$$

$$\equiv \sigma + k_s q^2 \ln(q \ell_k^{MD}) + \mathcal{O}(q^4), \tag{101}$$

where k_s and k_0 are given by the expressions in Eqs. (92) and (94), and where k_{MD} is given by the previously derived expression in Eq. (85) for SR forces. In Fig. 11, we show, as the dotted line, the result for the bending length ℓ_k^{MD}.

VII. DISCUSSION

In the first part of this article, we have demonstrated that the full spectrum of surface fluctuations obtained in MC simulations[3] of the colloid-polymer interface can very accurately be described by the following expression:

$$S(q) = \frac{k_B T}{\sigma q^2} - \frac{k k_B T}{\sigma^2} + \mathcal{N}_L S_b(q). \tag{102}$$

The three terms in this expression work in three different q-regimes:

(1)   classical CW regime, $qd \ll 1$,
(2)   ECW regime, $qd \lesssim 1$, and
(3)   bulklike fluctuation regime, $qd \gtrsim 1$.

Two adjustable parameters are present: $\mathcal{N}_L$ that weighs the bulklike fluctuations compared to the CW fluctuations and the bending rigidity k as defined by the leading order correction in an expansion of $\sigma(q)$ in q^2, $\sigma(q) = \sigma + kq^2 + \cdots$. We found that a fit to the simulation results yields $k < 0$, i.e., the leading order curvature correction tends to *lower* the surface tension $\sigma(q)$. This effect is termed *capillary enhancement*;[1] CWs are "more violent," less restricted by surface tension, at smaller wavelengths.

One could worry whether a negative bending rigidity is consistent with having a stable interface. Tarazona *et al.*[4] indicated that a decrease of $\sigma(q) = \sigma + kq^2 + \cdots$ ultimately

leads to a destabilization of the interface at *large* q. It is therefore important to realize that the extension of the CW model, through the inclusion of a bending rigidity, is valid only for *low* q. Higher order terms in the expansion in q are not systematically included. In this article we propose to describe $S(q)$ for large q ($qd \gtrsim 1$) in terms of molecular bulk-like fluctuations through $S_b(q)$. It is shown that the full $S(q)$, which is then a combination of the ECW model at low q and bulklike fluctuations at large q, remains well behaved ensuring the stability of the interface. For systems with a low (or even zero) surface tension, the bending rigidity is the dominant contribution near $q=0$ and one necessarily requires a positive value for k,[35] but for the simple, (quasi-) one-component system considered here this is not an issue.

A most important and generally underappreciated point that we like to emphasize is that the location of the interface cannot be defined *unambiguously*. A certain procedure must always be formulated to determine the height function $h(\vec{r}_{\parallel})$. We have shown that different choices for the location of the interface, which are all equally legitimate as long as they lead to a location of the dividing surface that is "sensibly coincident" with the interfacial region,[23] lead to different results for the bending correction to the CW model. Naturally, all *experimentally* measurable quantities *cannot* depend on the chosen location of the interface, making it necessary to formulate precisely the quantity that is determined in experiments or simulations. It was shown that for the simulation results, the value of the bending rigidity in the above expression for $S(q)$ corresponds to the height function being defined according to the ic, $k = k^{ic}$.

For the determination of k, it is necessary to take the contribution from bulklike fluctuations into account since they also contribute as a constant, $\mathcal{N}_L S_b(0)$, in the CW regime ($qd \ll 1$). This observation is consistent with the interpretation of light scattering results by Daillant and co-workers.[1] To determine $\sigma(q)$, they subtract from $S(q)$ a contribution proportional to the penetration depth ($\propto \mathcal{N}_L$) times the liquid compressibility [$\propto S_b(0)$]. Even though the light scattering results by Daillant and co-workers[1] are obtained for real fluids, for which the interaction potential is not necessarily SR, one expects that a description in terms of the above mentioned three regimes is again useful. A further comparison with the light scattering results is, however, necessary.

In the second part of this article, a molecular theory to describe the inclusion of the bending rigidity correction to the CW model is presented. An essential feature of the theory is the ansatz made in Eq. (53) regarding the thermodynamic conditions used to vary the interfacial curvature. It improves on earlier choices made in the sense that the bulk densities are equal to those at coexistence and the density profile is a continuous function.[21,22,24,30] The theory predicts that the scaling behavior of the bending rigidity equals that of the surface tension near the critical point

$$k \propto \sigma d^2 \propto t^{\mu}, \tag{103}$$

where $\mu \approx 1.26$ is the usual surface tension critical exponent (in mean-field $\mu = 3/2$).[7] This new scaling prediction differs fundamentally from the scaling of the bending rigidity in the "equilibrium approach," $k_{eq} \propto \sigma \xi^2$. In this approach the bending rigidity is determined from considering the equilibrium free energy of spherically and cylindrically shaped liquid droplets, with their radii varied by changing the value of the system's chemical potential.[20,25,36]

The negative sign and the scaling behavior of the bending rigidity obtained from the molecular theory are in accord with MC simulations. However, the magnitude of k from the molecular theory, $\sqrt{-k/\sigma} \approx 0.13d$, is significantly below the value obtained in the simulations, $\sqrt{-k/\sigma} \approx 0.47d$ (see also Fig. 8), but we believe this to be due to simplifications made in the theory rather than a true discrepancy.

ACKNOWLEDGMENTS

APPENDIX A: DEPLETION INTERACTION POTENTIAL

The phase-separated colloid-polymer system is effectively treated as a one-component system considering the colloids only. The colloid-colloid interaction is then given by a hard-sphere repulsion (diameter d) with an attractive depletion interaction[15] induced by the presence of polymers (radius R_g)

$$U_{dep}(r) = \frac{-k_B T \eta_p}{2(\varepsilon - 1)^3}\left[2\varepsilon^3 - 3\varepsilon^2\left(\frac{r}{d}\right) + \left(\frac{r}{d}\right)^3\right] \tag{A1}$$

with $d < r < \varepsilon d$ and the size ratio parameter ε is defined as

$$\varepsilon \equiv 1 + \frac{2R_g}{d}. \tag{A2}$$

Using this form for $U_{att}(r)$, the coefficients a, m, and B are readily calculated to yield

$$a = k_B T d^3 \eta_p \frac{\pi}{12}(2 + 6\varepsilon + 3\varepsilon^2 + \varepsilon^3),$$

$$m = k_B T d^5 \eta_p \frac{\pi}{240}(5 + 15\varepsilon + 10\varepsilon^2 + 6\varepsilon^3 + 3\varepsilon^4 + \varepsilon^5),$$

$$B = k_B T d^7 \eta_p \frac{\pi}{8400}(28 + 84\varepsilon + 63\varepsilon^2 + 45\varepsilon^3 + 30\varepsilon^4 + 18\varepsilon^5$$
$$+ 9\varepsilon^6 + 3\varepsilon^7). \tag{A3}$$

One may also determine the functions $w_0(z_{12})$, $w_2(z_{12})$, and $w_4(z_{12})$. When $|z_{12}| < d$ one has

$$w_0(z_{12}) = -k_B T d^2 \eta_p \frac{\pi}{5}(1 + 3\varepsilon + \varepsilon^2),$$

$$w_2(z_{12}) = k_\mathrm{B} T d^4 \eta_p \frac{\pi}{280} \left[10 + 30\varepsilon + 18\varepsilon^2 + 9\varepsilon^3 + 3\varepsilon^4 \right.$$
$$\left. - 14(1 + 3\varepsilon + \varepsilon^2)\frac{z_{12}^2}{d^2} \right],$$

$$w_4(z_{12}) = -k_\mathrm{B} T d^6 \eta_p \frac{\pi}{20\,160} \left[5(7 + 21\varepsilon + 15\varepsilon^2 + 10\varepsilon^3 \right.$$
$$+ 6\varepsilon^4 + 3\varepsilon^5 + \varepsilon^6) - 9(10 + 30\varepsilon + 18\varepsilon^2 + 9\varepsilon^3$$
$$\left. + 3\varepsilon^4)\frac{z_{12}^2}{d^2} + 63(1 + 3\varepsilon + \varepsilon^2)\frac{z_{12}^4}{d^4} \right]. \qquad \text{(A4)}$$

When $d < |z_{12}| < \varepsilon d$ one has

$$w_0(z_{12}) = \frac{-k_\mathrm{B} T d^2 \eta_p}{(\varepsilon - 1)^3} \frac{\pi}{5} \left[\varepsilon^5 - 5\varepsilon^3\frac{z_{12}^2}{d^2} + 5\varepsilon^2\frac{|z_{12}|^3}{d^3} - \frac{|z_{12}|^5}{d^5} \right],$$

$$w_2(z_{12}) = \frac{k_\mathrm{B} T d^4 \eta_p}{(\varepsilon - 1)^3} \frac{\pi}{280} \left[3\varepsilon^7 - 14\varepsilon^5\frac{z_{12}^2}{d^2} + 35\varepsilon^3\frac{z_{12}^4}{d^4} \right.$$
$$\left. - 28\varepsilon^2\frac{|z_{12}|^5}{d^5} + 4\frac{|z_{12}|^7}{d^7} \right],$$

$$w_4(z_{12}) = \frac{-k_\mathrm{B} T d^6 \eta_p}{(\varepsilon - 1)^3} \frac{\pi}{20\,160} \left[5\varepsilon^9 - 27\varepsilon^7\frac{z_{12}^2}{d^2} + 63\varepsilon^5\frac{z_{12}^4}{d^4} \right.$$
$$\left. - 105\varepsilon^3\frac{z_{12}^6}{d^6} + 72\varepsilon^2\frac{|z_{12}|^7}{d^7} - 8\frac{|z_{12}|^9}{d^9} \right]. \qquad \text{(A5)}$$

APPENDIX B: LONDON-DISPERSION FORCES

The following explicit form for $U_\mathrm{att}(r)$ is considered:

$$U_\mathrm{att}(r) = \begin{cases} -A/r^6 & \text{when} \quad r > d \\ 0 & \text{when} \quad r < d. \end{cases} \qquad \text{(B1)}$$

Using this form for $U_\mathrm{att}(r)$, the coefficients a and m are readily calculated to yield

$$a = \frac{2\pi A}{3d^3} \quad \text{and} \quad m = \frac{\pi A}{3d}. \qquad \text{(B2)}$$

With this form for the interaction potential one may expand $\omega(q, z_{12})$. When $|z_{12}| > d$ one has

$$\omega(q, z_{12}) = -\frac{\pi A}{2z_{12}^4} + \frac{\pi A}{8z_{12}^2}q^2 + \frac{\pi A}{32}q^4 \ln(qd)$$
$$+ \frac{\pi A}{32}q^4 \left[\gamma_E - \frac{3}{4} + \frac{1}{2}\ln\left(\frac{z_{12}^2}{4d^2}\right) \right] + \cdots. \qquad \text{(B3)}$$

When $|z_{12}| < d$ one has

$$\omega(q, z_{12}) = -\frac{\pi A}{2d^4} + \frac{\pi A}{8d^2}\left(2 - \frac{z_{12}^2}{d^2}\right)q^2 + \frac{\pi A}{32}q^4 \ln(qd)$$
$$+ \frac{\pi A}{32}q^4 \left[\gamma_E - \frac{3}{2} - \ln(2) + \frac{z_{12}^2}{d^2} - \frac{z_{12}^4}{4d^4} \right] + \cdots. \qquad \text{(B4)}$$

[1] C. Fradin, A. Braslau, D. Luzet, D. Smilgies, M. Alba, N. Boudet, K. Mecke, and J. Daillant, Nature (London) **403**, 871 (2000); J. Daillant and M. Alba, Rep. Prog. Phys. **63**, 1725 (2000); S. Mora, J. Daillant, K. Mecke, D. Luzet, A. Braslau, M. Alba, and B. Struth, Phys. Rev. Lett. **90**, 216101 (2003).

[2] J. Stecki and S. Toxvaerd, J. Chem. Phys. **103**, 9763 (1995).

[3] R. L. C. Vink, J. Horbach, and K. Binder, J. Chem. Phys. **122**, 134905 (2005).

[4] P. Tarazona, R. Checa, and E. Chacon, Phys. Rev. Lett. **99**, 196101 (2007).

[5] R. Evans, in *Liquids at Interfaces, Les Houches XLVIII (1988)*, edited by J. Charvolin, J. F. Joanny, and J. Zinn-Justin (North-Holland, Amsterdam, 1990).

[6] J. R. Henderson, in *Fundamentals of Inhomogeneous Fluids*, edited by D. Henderson (Dekker, New York, 1992).

[7] J. S. Rowlinson and B. Widom, *Molecular Theory of Capillarity* (Clarendon, Oxford, 1982).

[8] F. P. Buff, R. A. Lovett, and F. H. Stillinger, Phys. Rev. Lett. **15**, 621 (1965).

[9] J. D. Weeks, J. Chem. Phys. **67**, 3106 (1977).

[10] D. Bedeaux and J. D. Weeks, J. Chem. Phys. **82**, 972 (1985).

[11] W. Helfrich, Z. Naturforsch [C] **28C**, 693 (1973).

[12] J. Meunier, J. Phys. **48**, 1819 (1987); H. Kellay, B. P. Binks, and J. Meunier, Phys. Rev. Lett. **70**, 1485 (1993); H. Kellay and J. Meunier, J. Phys.: Condens. Matter **8**, A49 (1996).

[13] E. M. Blokhuis and D. Bedeaux, Physica A **164**, 515 (1990); J. W. Schmidt, Phys. Rev. A **38**, 567 (1988).

[14] E. M. Blokhuis, J. Kuipers, and R. L. C. Vink, Phys. Rev. Lett. **101**, 086101 (2008).

[15] S. Asakura and F. Oosawa, J. Chem. Phys. **22**, 1255 (1954); A. Vrij, Pure Appl. Chem. **48**, 471 (1976).

[16] A. P. Gast, C. K. Hall, and W. B. Russel, J. Colloid Interface Sci. **96**, 251 (1983).

[17] H. N. W. Lekkerkerker, W. C. K. Poon, P. N. Pusey, A. Stroobants, and P. B. Warren, Europhys. Lett. **20**, 559 (1992).

[18] D. G. A. L. Aarts and H. N. W. Lekkerkerker, J. Phys.: Condens. Matter **16**, S4231 (2004); D. G. A. L. Aarts, M. Schmidt, and H. N. W. Lekkerkerker, Science **304**, 847 (2004).

[19] K. R. Mecke and S. Dietrich, Phys. Rev. E **59**, 6766 (1999).

[20] E. M. Blokhuis and D. Bedeaux, Mol. Phys. **80**, 705 (1993).

[21] A. O. Parry and C. J. Boulter, J. Phys.: Condens. Matter **6**, 7199 (1994).

[22] E. M. Blokhuis, J. Groenewold, and D. Bedeaux, Mol. Phys. **96**, 397 (1999).

[23] J. W. Gibbs, *Collected Works* (Dover, New York, 1961).

[24] E. M. Blokhuis and D. Bedeaux, Physica A **184**, 42 (1992); E. M. Blokhuis and D. Bedeaux, Heterog. Chem. Rev. **1**, 55 (1994).

[25] G. Gompper and S. Zschocke, Phys. Rev. A **46**, 4836 (1992); G. Gompper and M. Schick, in *Self-Assembling Amphiphilic System*, Phase Transitions and Critical Phenomena Vol. 16, edited by C. Domb and J. Lebowitz (Academic, London, 1994).

[26] J. K. Percus and G. J. Yevick, Phys. Rev. **110**, 1 (1958).

[27] A. O. Parry, C. Rascón, N. R. Bernardino, and J. M. Romero-Enrique, Phys. Rev. Lett. **100**, 136105 (2008); **18**, 6433 (2006); **19**, 416105 (2007).

[28] H. N. W. Lekkerkerker, Colloids Surf. **51**, 419 (1990).

[29] N. F. Carnahan and K. E. Starling, J. Chem. Phys. **51**, 635 (1969).

[30] M. E. Fisher and A. J. Jin, Phys. Rev. B **44**, 1430 (1991); Phys. Rev. Lett. **69**, 792 (1992); A. J. Jin and M. E. Fisher, Phys. Rev. B **47**, 7365 (1993).

[31] J. Kuipers and E. M. Blokhuis, J. Colloid Interface Sci. **315**, 270 (2007).

[32] C. Varea and A. Robledo, Mol. Phys. **85**, 477 (1995).

[33] M. Napiórkowski and S. Dietrich, Phys. Rev. E **47**, 1836 (1993); M. Napiórkowski and S. Dietrich, Z. Phys. B: Condens. Matter **97**, 511 (1995).

[34] R. H. Fowler, Proc. R. Soc. London, Ser. A **159**, 229 (1937).

[35] S. A. Safran, *Statistical Thermodynamics of Surfaces, Interfaces and Membranes* (Addison-Wesley, Reading, MA, 1994).

[36] A. E. van Giessen and E. M. Blokhuis, J. Chem. Phys. **116**, 302 (2002).